Effect of dislocations on electrical and electron transport properties of InN thin films. II. Density and mobility of the carriers

V. Lebedev,[a] V. Cimalla, T. Baumann, and O. Ambacher
Center for Micro- and Nanotechnologies, Technical University Ilmenau, D-98684 Ilmenau, Germany

F. M. Morales,[b] J. G. Lozano, and D. González.
Departamento de Ciencia de los Materiales e Ingeniería Metalúrgica y Química Inorgánica, Facultad de Ciencias, Universidad de Cádiz, 11510 Puerto Real, Cádiz, Spain

(Received 14 March 2006; accepted 25 July 2006; published online 7 November 2006)

The influence of dislocations on electron transport properties of undoped InN thin films grown by molecular-beam epitaxy on AlN(0001) pseudosubstrates is reported. The microstructure and the electron transport in InN(0001) films of varying thickness were analyzed by transmission electron microscopy and variable temperature Hall-effect measurements. It was found that crystal defects have strong effects on the electron concentration and mobility of the carriers in the films. In particular, the combined analysis of microscopy and Hall data showed a direct dependence between free carrier and dislocation densities in InN. It was demonstrated that threading dislocations are active suppliers of the electrons and an exponential decay of their density with the thickness implies the corresponding decay in the carrier density. The analysis of the electron transport yields also a temperature-independent carrier concentration, which indicates degenerate donor levels in the narrow band-gap InN material. The relative insensitivity of the mobility with respect to the temperature suggests that a temperature-independent dislocation strain field scattering dominates over ionized impurity/defect and phonon scattering causing the increase of the mobility with rising layer thickness due to the reducing dislocation density. Room temperature mobilities in excess of 1500 $cm^2\ V^{-1}\ s^{-1}$ were obtained for ~800 nm thick InN layers with the dislocation densities of $\sim 3\times 10^9\ cm^{-2}$. © *2006 American Institute of Physics*. [DOI: 10.1063/1.2363234]

I. INTRODUCTION

A narrow band gap (~0.7 eV) (Refs. 1–7) and superior electron transport properties (e.g., low effective mass, high predicted electron mobility of ~4400 $cm^2\ V^{-1}\ s^{-1}$ at 300 K, and saturation drift velocity) make InN a very attractive material for high-frequency electronic devices[8–11] and near-infrared optoelectronics.[12–17] However, InN device technology is still hampered by many factors including the absence of a suitable lattice matched substrate and a low dissociation temperature of InN. In order to realize these promising devices, the ability to grow InN-based heterostructures with high crystalline quality remains the most critical technological challenge.

Despite of the large differences in lattice constants (~14% for InN/AlN and ~11% for InN/GaN), considerable effort has been devoted to grow high quality InN on other III-nitride epitaxial layers by plasma induced molecular-beam epitaxy.[15,18–24] (PIMBE) and metal-organic chemical vapor deposition.[25–29] It has been proposed earlier[30] and experimentally demonstrated in the first part of the paper that the strain in epitaxial InN/$Al_xGa_{1-x}N$ heterosystems is initially relieved by misfit dislocations and by surface islanding. Threading dislocations (TDs), which arise in the epilayer as a consequence of domain coalescence and plastic relaxation, have been reported to have a deleterious impact on the electronic properties of III-nitride material. Specifically, such dislocations act as nonradiative recombination centers in GaN and AlN (Refs. 31 and 32) and other direct band-gap semiconductors, severely degrading light emission efficiency. Recently, TDs have been reported to reduce electron mobility in GaN/AlGaN field effect transistor structures.[33,34]

While dislocations in GaN and Ga-rich GaInN were extensively studied, few works have been published on dislocation characterization[6,21,35] and on the impact of dislocation on the electron transport in InN epilayers.[24,36–38] Previously, transport studies were performed on InN grown mainly on III-nitride epitaxial templates.[35,36,39,40] However, detailed microstructure characterization and a correlation with electrical properties have been rarely attempted.

In this work, we discuss the influence of structural growth defects on electron transport properties of undoped InN thin films grown by PIMBE on AlN(0001)/sapphire pseudosubstrates. The results of variable temperature Hall-effect and transmission electron microscopy (TEM) measurements have been analyzed to obtain the information associating the microstructure and electron transport in heteroepitaxial InN films with varying thickness. It will be shown that the threading dislocation density varies with epilayer thickness affecting both the carrier concentration and electron mobility resulting in a direct dependence between carrier generation and dislocation density in InN films. Additionally, it will be also demonstrated that a dislocation strain field scattering dominates over other scattering mechanisms in the investigated epilayers.

[a]Electronic mail: vadim.lebedev@tu-ilmenau.de
[b]Also at the Center for Micro- and Nanotechnolgies of TU-Ilmenau.

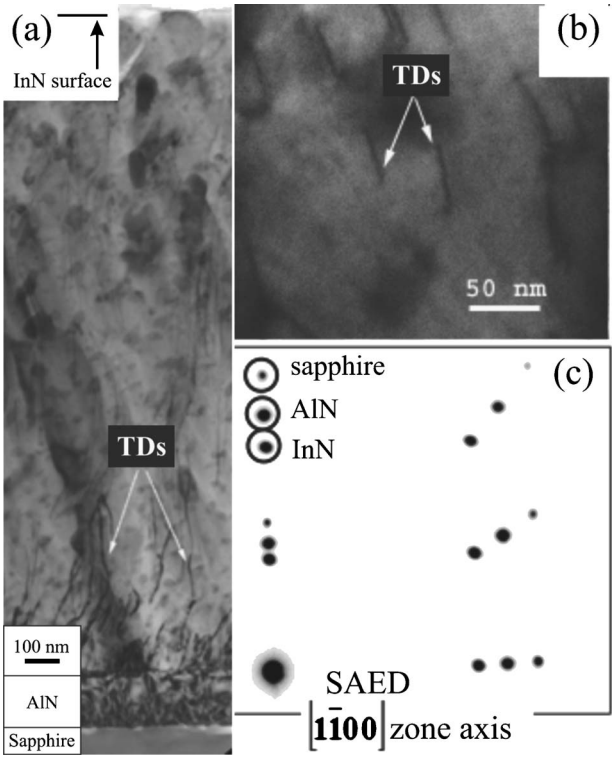

FIG. 1. (a) Bright-field XTEM micrograph taken under two beam conditions using the (0002) reflection of InN near the $\langle 11\bar{2}0\rangle$ zone axis. (b) PVTEM micrograph recorded under two beam conditions near the [0001] zone axis of InN using the $(11\bar{2}0)$ reflection and (c) SAED pattern of a 760 nm thick 2*H*-InN/2*H*-AlN/Al_2O_3 heterostructure registered when sapphire is orientated along the $[1\bar{1}00]$ direction. The encircled spots stand for 0002 aligned reflections of layers and substrate, indicating good epitaxy relationship.

II. EXPERIMENT

The growths of epitaxial wurtzite (2*H*) AlN(0001) template and 2*H*-InN epilayers were performed in a turbopumped Balzer's PIMBE chamber with a background pressure of 2×10^{-10} mbar, conventional effusion cells, and an Oxford applied research rf plasma source for generation of nitrogen radicals. The AlN growth was anticipated by a nitridation of $Al_2O_3(0001)$ wafers at a temperature of 1100 °C for 2 min. Next, a 200–250 nm thick AlN buffer layer was deposited at 900 °C to form an epitaxial template for the InN growth [see Fig. 1(a)]. The detailed description of the growth conditions and results on x-ray and electron microscopy studies of dislocations networks in 2*H*-InN samples have been considered in the first part of the paper. Microstructural characterization was performed using both Technai 20 S-TWIN and JEOL 2011 transmission electron microscopes with accelerating voltages of 200 kV. Cross-section TEM (XTEM) and plan-view TEM (PVTEM) imagings were used to study the distribution of dislocations in the epilayer.

Hall-effect measurements have been routinely used to obtain type, concentration, and mobility of the carriers. From measurements of the Hall coefficient R_S and the conductivity σ_S, the Hall mobility μ and the Hall sheet carrier concentration N_S were calculated at each temperature. Additionally, the variation of mobility with temperature was used to yield information on competing scattering mechanisms. The measurements were performed using the van der Pauw technique. Square specimens were cleaved and indium contacts were soldered at the four corners of the sample at 200 °C. Hall measurements were then performed over the temperature range from 100 to 300 K at 0.4 T. The temperature and the magnetic field were controlled by a Accent HL5500 system. The sign of the Hall coefficient indicated that the majority carriers were electrons for every sample.

III. EXPERIMENTAL RESULTS

In Fig. 1(a), a typical bright-field XTEM micrograph of a 2.2 μm InN layer grown on AlN/$Al_2O_3(0001)$ epitaxial template is shown. The micrograph has been taken in two beam conditions using the (0002) reflection of InN near the $[11\bar{2}0]$ zone axis. The nonuniformity of the dislocation microstructure is apparent. The defect density is very high in the near-interface region and decreases with increasing distance from the interface being the greatest variation in the initial of 10–200 nm. Figure 1(b) is a PVTEM micrograph of the same sample, from which the near-surface InN threading defect density is estimated to be $\sim3\times10^9$ cm^{-2}. Selective area electron diffraction (SAED) pattern shown in Fig. 1(c) demonstrates the following heteroepitaxial relationship: $[1\bar{1}00]Al_2O_3\|[2\bar{1}\bar{1}0]AlN\|[2\bar{1}\bar{1}0]InN$.

Figure 2(a) shows the variations of the Hall sheet carrier density, $N_s=(qR_s)^{-1}$, against temperature for the samples of different thicknesses ranging from 650 to 2200 nm, where R_s is the Hall coefficient. As one can see, N_s varies strong from sample to sample for thinner InN layers, but only slightly for thicker InN. This suggests a very high interfacial contribution and a drop to a lower background bulk value as a sample thickness increases. Figure 2(b) shows the mobility, $\mu=R_s\sigma_s$, as a function of temperature for the set of InN samples of variable thickness, where σ_s is the zero field conductivity. The mobility clearly increases with sample thickness and shows only small temperature dependence for thinner samples. For thicker samples, a very broad maximum occurs near ~160 K.

The obtained temperature dependencies of $\mu(T)$ and $N_s(T)$ (Fig. 2) are qualitatively very similar to those observed for InAs epilayers.[41] In general, the unpronounced dependence $N_s(T)$ reflects the fact that N_s is a function of the carrier density weighted by the mobility, but does not indicate thermal activation of the carriers in the bulk, which is characteristic for GaN epilayers. Moreover, a very weak temperature dependence of N_s suggests that the existing defect levels responsible for the carrier generation are degenerated,[24,36,39] similar to those observed in InAs.[41] The existence of degeneracy in InN with $N_S>10^{18}$ cm^{-3} has been predicted by the calculated concentration at the Mott transition, about 4×10^{16} cm^{-3}.[36]

Figure 3(a) plots measured carrier density n_e (open rectangles) as a function of the sample thickness. There is a steep drop in the carrier concentration away from the interface. The thickness variation of n_e shows the same general trend as the threading dislocation density versus thickness. Initially, a very high dislocation density of $N_{TD}\sim4\times10^{11}$ cm^{-2} exists near the interface. With a rising thickness, the dislocation density follows an exponential decay law and

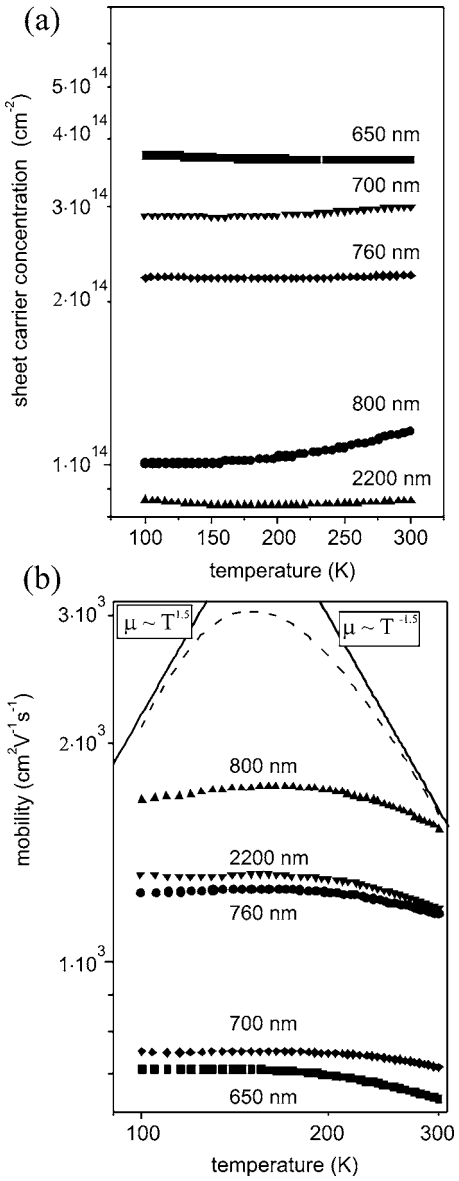

FIG. 2. Variation of (a) the sheet carrier density and (b) the Hall mobility with temperature for a set of InN samples of variable thickness. The dashed line represents the bulk mobility dependence on temperature, $\mu_0(T)$, for the 800 nm thick sample fitted by Eq. (7).

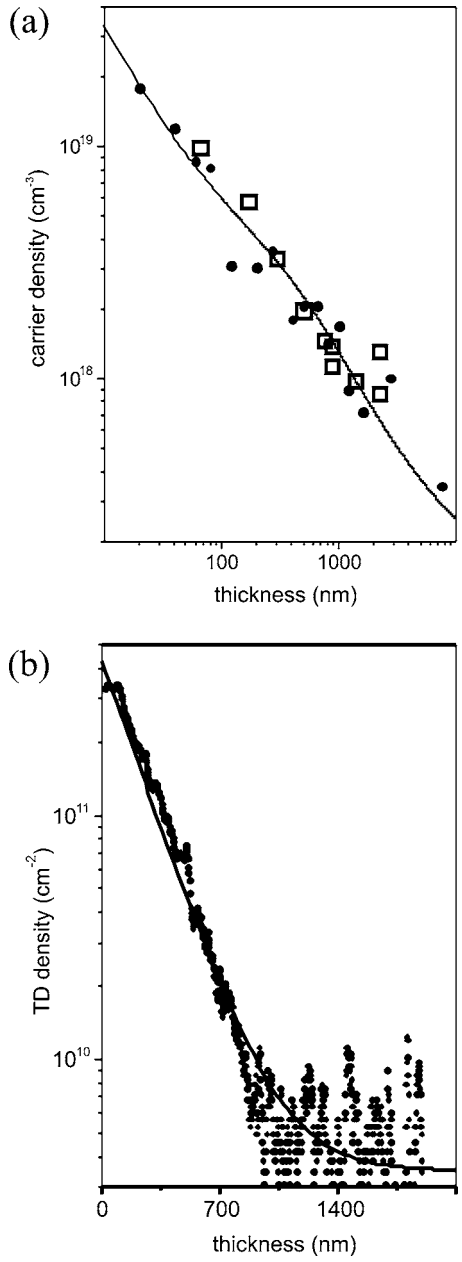

FIG. 3. (a) The Hall carrier density variations vs thickness for a set of InN epilayers (open rectangles). The solid line is an experimental fit based on Eq. (6). The black circles represent the data published by Lu *et al.* (Ref. 37). (b) The TD density as a function of the epilayer thickness (black circles). The TD distribution has been taken from ~2.2 μm InN epilayer grown on AlN(0001). The solid line represents an experimental fit using Eq. (3).

also reaches a limiting value of $\sim 3\times 10^9$ cm^{-2} far from the interface ($\sim$2.2 μm) [see Fig. 3(b) and details in the first part of this paper]. Both dependencies can be fitted by a similar exponential decay function $[y(d)=\alpha+\beta\exp(-d/\gamma)]$ of thickness d in the range of 0.6–2.2 μm,

$$N_{\mathrm{TD}}(d) = 3.5\times 10^9 + 4\times 10^{11}\exp(-d/\gamma_1)\ (\mathrm{cm}^{-2}), \quad (1)$$

$$n_e(d) = 5\times 10^{17} + 5\times 10^{19}\exp(-d/\gamma_2)\ (\mathrm{cm}^{-3}). \quad (2)$$

In this fit, the parameter α represents the lowest reachable value of the dislocation density in Eq. (1), and the background carrier concentration in the bulk in Eq. (2) for thicker ($\sim$2.2 μm) layers. In Eq. (2), α is the sum of the intrinsic and defect-generated carrier densities. The values of β show the top limit for the concentration of defects and free carriers for ultrathin InN epilayers. Parameter γ in Eq. (1) reflects the dynamic of the structural improvements in the epilayer, in particular, the drop in the defect density over the epilayer cross section. It is obvious, that γ is a function of many parameters, which are mainly related to the growth conditions and the strain relief at the first phase of the growth. In general, every sample can exhibit its own unique γ value reflecting either favorable or unfavorable conditions for the epitaxy. In our case, we can assume that due to the identical growth conditions, all the samples have a similar dislocation distribution over the thickness. Therefore, certain conclusions can be drown based on the similarities in $N_{\mathrm{TD}}(d)$ and $n_e(d)$ dependencies. This question will be discussed in Sec. IV.

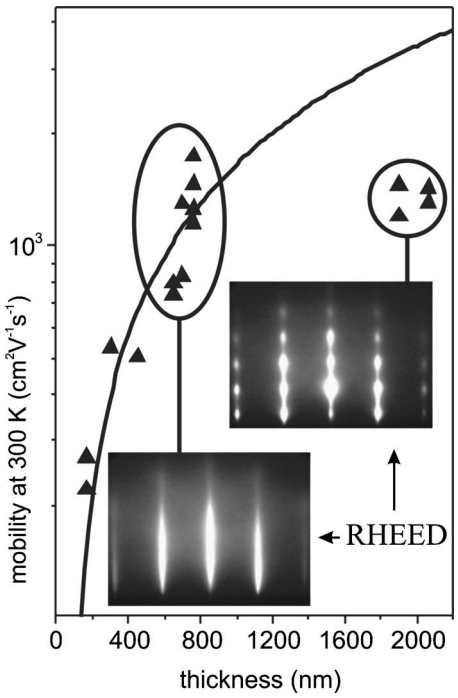

FIG. 4. Variation of the Hall mobility with the thickness of InN epilayers. Insets: *in situ* reflection high energy electron diffraction (RHEED) patterns.

Figure 4 plots μ as a function of the sample thickness at 300 K. The mobility increases with thickness following an exponential law. A fit of experimental data using exponential growth $\mu(d)=-\alpha+\beta\exp(d/\gamma)$ appears to saturate for a value in excess of the theoretical limit $\mu_{\max}\sim 4400\ \mathrm{cm^2\ V^{-1}\ s^{-1}}$ at thickness >2 μm. It is important to note that rising biaxial residual stress in the growing epilayer induces a Volmer-Weber growth mode after a certain critical thickness d_{3D} is reached. The similar behavior was observed also in 2*H*-AlN(0001)/Si(111) heterostructures[42] for epilayers thickness >1.2 μm. The reduction in mobility observed for ~ 2 μm thick 2*H*-InN samples is obviously determined by the lowering of the crystal quality due to the two dimensional→three dimensional growth transition (see diffraction patterns in Fig. 4) observed at a thickness of $d_{3D}\sim 1.6$ μm for the samples grown on AlN(0001) templates.

IV. DISCUSSION

It is important to note that the interpretation of the Hall data in InN is extremely complicated due to the micro- and macrostructural nonuniformity, i.e., domain structure of the film, stochiometry fluctuations, segregation processes, etc. Moreover, the Fermi level of the free surface in InN is known to be pinned in the conduction band,[43] resulting in a surface carrier accumulation similar to the case of InAs.[41,44]

In a nonuniform layer where the mobility and carrier concentration vary with thickness, the standard interpretation of Hall-effect data provides a weighted average value of these quantities,

$$N_S=\frac{1}{qR_S}=\frac{\left[\int_0^d n(x)\mu(x)dx\right]^2}{\int_0^d n(x)\mu^2(x)dx}, \tag{3}$$

$$\mu=R_S\sigma_S=\frac{\int_0^d n(x)\mu^2(x)dx}{\int_0^d n(x)\mu(x)dx}. \tag{4}$$

The true sheet carrier density and the average mobility can differ considerably from the measured values, especially, for thin epilayers. It was shown by variable field Hall measurements that InN has, in fact, a layered structure with areas of differing electron concentrations and Hall mobilities, which are averaged by a simple Hall analysis. In this case, the large gradient in mobility could cause measured N_s to be dominated by a small fraction of carriers having a higher mobility determining an "effective cross section" for the conduction. On the other hand, the known strong accumulation of electrons at the surface[45,46] will superimpose measurements of the carrier concentration, especially in the case of thin InN films. Additionally, in thin epilayers, besides the bulk and surface carrier generation, other mechanisms of the carrier generation can play a significant role, i.e., the high interfacial sheet carrier density could be caused by a structural donor source as for the case of InAs (Ref. 41) or/and vacancy- or impurity-related mechanisms. In the following discussion, we intentionally restrict our consideration by relatively thick 2*H*-InN samples. In particular, an impact of the dislocation density on the concentration and mobility of the carriers will be considered for the samples with thickness ranging from 350 to 2200 nm.

A. Impact of the dislocation density on the carrier concentration

Recently presented results have demonstrated direct evidences that the dislocations of edge, screw, and mixed characters in *n*-type GaN are negatively charged. It was proposed that acceptor-type Ga vacancies presented in the core of TD yield ~ 2 acceptors per 1 nm along the dislocation.[47,49–54] Previous studies of 2*H*-InN considered negatively charged dislocations by analogy with GaN.[24,36] However, in view of the revision of the band gap, positively charged donor nitrogen vacancies along dislocations are now considered to be energetically favorable for *n*-type InN.[55]

In our case, identical best-fit values of $\gamma\sim\gamma_1\sim\gamma_2\sim 238\pm 10$ nm and the equal proportion of the limiting values α and β in Eqs. (1) and (2) indicate that the carrier generation is obviously defect related. Thus, a quantitative model of a bulk carrier generation in InN can be derived based on the following assumptions.

- An exponential decay in the dislocation density profile [given by Eq. (1) and shown in Fig. 3(b)] has a universal character reflecting a TD recombination dynamic for the actual growth conditions.
- A full core dislocation model[47–50] can be applied to describe an internal core structure of threading *edge-type and mixed-character* dislocations in 2*H*-InN(0001),
- a noncomplete ionization of atoms along the dislocation core takes place yielding of ~ 1 electron per $\lambda=2c_{\mathrm{InN}}$ of dislocation length in 2*H*-InN.

Therefore, the contribution of the TD-induced electrons to the total free carrier density as a function of the epilayer thickness can be estimated using an empirical formula,

$$n_e^{\mathrm{TD}} = \frac{1}{d}\sum_{i=1}^{k} N_i^{\mathrm{TD}} = \frac{1}{d}\sum_{i=1}^{k} (\alpha + \beta e^{-(i\lambda)/\gamma}) \ (\mathrm{cm}^{-3}), \tag{5}$$

where d is the total thickness of the epilayer and $k=d/\lambda$. However, this curve reproduces the experimentally obtained Hall carrier concentration dependence only for a limited range of thickness. The quantitative correlations for thinner (<300 nm) and for thicker (>2 μm) epilayers are rather poor.

The main reason for this discrepancy is the strong accumulation of electrons at the surface of InN. This surface accumulation is an intrinsic property of InN and has its origin in the extraordinary low conduction band minimum at the Γ point,[45] which allows donor-type surface states to be located inside the conduction band. As a consequence, on clean[45] and on air-exposed[46] InN surfaces, a localized sheet carrier density of about $N_L \sim 2.5\times10^{13}$ cm^{-2} is generated. These free electrons affect the apparent electron concentration n_e, measured by Hall effect. Thus, a general model of carrier generation in InN epilayers has to include at least three independent components;

$$n_e = n_{\mathrm{point}} + \frac{N_L}{d} + n_e^{\mathrm{TD}} \ (\mathrm{cm}^{-3}), \tag{6}$$

where n_{point} is the background carrier density of about 1×10^{17} cm^{-3},[56,57] which is a sum of intrinsic, impurity- and point-defect-generated carrier concentrations in the thick epilayers. A model fit is presented in Fig. 3(a) by a solid line. The black circles representing the data published by Lu *et al.*[37] have been used as a reference. The fit of the data shows an excellent agreement for $\lambda \sim 1.1$ nm. Here, we have to point out that the assumption of the noncomplete ionization of atoms along the dislocation line gives an uncertainty factor in the numerical estimations. Mixed character of the TDs also plays a role reducing the number of the defect-generated electrons.

B. Variation of mobility with temperature and thickness

Among the possible scattering mechanisms limiting the mobility in epilayers, neutral impurity scattering μ_N,[58] ionized impurity scattering μ_I,[59] polar optical phonon scattering μ_{PO},[60] acoustic deformation potential scattering μ_{DP},[58] piezoelectric potential scattering μ_{PE},[55] and structural imperfection scattering μ_D (Refs. 41, 52, 61, and 62) have been studied in detail. According to Matthiesen's rule, we can express the total mobility as $1/\mu = \Sigma_i 1/\mu_i$, where i accounts for all scattering mechanisms mentioned above. It is commonly accepted that there are two most important mechanisms limiting the carrier mobility in semiconductors—ionized impurity scattering and phonon scattering.[36,63–65] It was shown that these mechanisms exhibit certain temperature dependences: $\mu_I(T) \sim T^{1.5}$ for the ionized impurity scattering at low temperature region ($T<100$ K) and $\mu_P(T) \sim T^{-1.5}$ for phonon scattering characteristic for higher temperatures.[65,66]

The temperature dependencies of the Hall mobility in high-quality InN epilayers have been analyzed recently by Thakur *et al.*[24] In our report, we will restrict our consideration to a general discussion of the experimentally obtained results with a particular emphasis on contributions of the dislocation scattering. As one can see, the weak temperature dependence shown in Fig. 2(b) exhibits power-law exponents much smaller than 1.5. For the most sensitive with respect to the temperature variations sample, the low temperature and the high temperature exponents are ~0.1 and is ~0.3, respectively. Thus, the observed relative temperature insensitivity of μ presumes the dominance of the scattering mechanism with a weak dependency on the temperature—either the neutral impurity scattering μ_N or the structural imperfection scattering μ_D.

Neutral impurities (neutral vacancies and isoelectronic substitutional elements) are believed to cause temperature-independent scattering in conventional semiconductors.[63] For instance, in AlN:Si epilayers, the mobility limited by the neutral impurity scattering was found to be the lowest among the other scattering mechanisms.[66] It was shown that due to the high density of donors and large donor activation energy in AlN:Si, a few donors are ionized but almost all of them are neutral impurities. However, it was demonstrated that InN possesses highly degenerated donor levels.[36,39] This follows also from our temperature-dependent Hall data. As a result, all the donor sites have to be ionized and almost all of them become charged impurities, which should exhibit $\mu_I(T) \sim T^{1.5}$ at a low temperature region if they dominate.

Also, surface and interface roughness, as well as structural micro- and macrodefects, inhomogeneously distributed in the bulk limit the free carrier mean free path, especially in the epilayers with pronounced domain structure (i.e., grown in the mode close to Volmer-Weber conditions). All of them are not expected to have explicit temperature dependence.[67] Atomic force microscopy (AFM) measurements indicate that the surface roughness of the InN epilayers does not vary much for the thicknesses higher than 300 nm being of ~2 nm (a root mean square value for 5×5 μm^2 scan). If surface roughness would account for the lower mobility of the very thin samples roughness related scattering is not a major contributor for the thicker samples due to the larger volume available for the conduction.

According to the TEM analyses [Fig. 1(a)], the density of TDs decreases with increasing thickness, whereas the average spacing of TDs increases. Simultaneously, the Hall-effect measurements showed that the electron concentration decreases and the mobility increases with the rising film thickness. These phenomena can be attributed either to the scattering of electrons by crystal defects or to the effect of a native space charge region at the near-surface region of the films due to the presence of surface states.[62]

The concentration of charge at the near surface can also act as a scattering center due to the band bending and energy difference between bulk and surface electrons. However, this effect can be observed only in thin epilayers. Thus, the observed difference in transport properties of the films with

different thicknesses should be caused by the interaction between electrons and crystal defects such as TDs. Firstly, they act as scattering centers for electrons[68,69] due to the distortion of the crystal lattice near the defects, which decreases the mobility of the electrons. Misfit dislocations also create a potential well at their cores and electrical barriers besides the wells, which reduce the electron mobility, especially at the near-interface region. However, this effect becomes more pronounced for thinner films. In addition, the dislocation lines can become negatively charged scattering the electrons travelling across them and reducing the mobility. The impact of charged dislocation on electron mobility in GaN epilayers has been investigated by several groups.[52,53] In these reports, the most significant decrease of the mobility at lower carrier concentrations was attributed to the scattering of electrons by charges at threading dislocations, which act as Coulomb scattering centers. On the other hand, as one can see in Fig. 2(b), the ionized impurity and phonon scattering play more significant role in the thicker films following the same trend as the reduction in the defect density.[24]

For a highly dislocated material, the mobility μ ought to be corrected by an imperfection factor similar to that used in materials with domain boundaries,[51,62,69]

$$\mu = \mu_0\{1 + CN_{\mathrm{TD}} \exp(q\Phi_f/kT)\}^{-1}, \tag{7}$$

where C is constant, q is the electron charge, Φ_f is the potential at the dislocation,[70,71] and μ_0 is the bulk mobility: $\mu_0^{-1}(T)=\mu_I^{-1}(T)+\mu_P^{-1}(T)$. Since Φ_f and C are unknown, Eq. (7) does not allow a direct derivation of the bulk mobility. However, by using Eq. (7) in the parametrical fit for $\mu(T)$, and Φ_f and C as the fit parameters, the approximated dependence $\mu_0(T)$ can be derived. In Fig. 2(b), the dashed line represents $\mu_0(T)$ for the 800 nm thick sample with the best-fit value for $q\Phi_f$ of ~14 meV. It is comparable to the value of a potential barrier height of ~20 meV determined for GaN films by Fehrer *et al.*[71] using the same model.

C. Impact of impurities and point defects on mobility and density of the carriers

It has been shown that for degenerate electrons in InN at low temperatures, the only important scattering mechanisms are dislocation scattering and ionized point-defect/impurity scattering.[36] Using the formalism suggested by Look *et al.*,[61] one can determine donor (N_D) and acceptor (N_A) concentrations in degenerate semiconductor films. Under these circumstances, Eq. (6) can be modified to the form

$$1/\mu = 1/\mu_I + 1/\mu_D, \tag{8}$$

where

$$\mu_D = \frac{4\cdot 3^{2/3} e c^2 n^{2/3}}{\pi^{8/3}\hbar N_{\mathrm{TD}}}[1+y(n)]^{3/2}, \tag{9}$$

$$\mu_I = \frac{24\pi^3\varepsilon^2\hbar^3 n}{e^3 m^{*2} N_I\{\ln[1+y(n)] - y(n)/[1+y(n)]\}}, \tag{10}$$

$$y(n) = \frac{2\cdot 3^{1/3}\pi^{8/3}\varepsilon\hbar^2 n^{1/3}}{e^2 m^*}, \tag{11}$$

n is the measured carrier density, N_I is the density of ionized impurities and point defects, $m^* \sim 0.11 m_0$ is the effective mass, $\varepsilon \sim 15.3\varepsilon_0$ is the static dielectric constant, and c is the lattice constant (~5.71 Å). For $n > 10^{18}$ cm^{-3}, it was assumed that all donors are ionized even at low temperature.[36] Then, from the charge balance including the contribution of the charged centers at the dislocation lines one can write

$$\left.\begin{aligned} N_D - N_A + N_D^{\mathrm{TD}}(d) &= n(d) \\ N_D + N_A &= N_I - N_D^{\mathrm{TD}}(d) \end{aligned}\right\} \Rightarrow (N_A, N_D), \tag{12}$$

where $N_D^{\mathrm{TD}} \cong n_e^{\mathrm{TD}}$ is the volume density of the ionized centers in the TD cores. For the sample most sensitive to the temperature variation with $d=760$ nm, $\mu=1755$ cm^2 V^{-1} s^{-1}, $n=1.49\times10^{18}$ cm^{-3} at 160 K, and $N_{\mathrm{TD}} \sim 5\times10^9$ cm^{-2}, the calculated numbers are $N_D=1.1\times10^{18}$ cm^{-2} and $N_A=6.5\times10^{17}$ cm^{-2}, with the compensation ratio $\vartheta=N_A/(N_D+N_A)$ of ~0.37. ϑ values of the same order have been derived from the fitting of the charge neutrality equation for compensated n-type semiconductors,[66]

$$\frac{n(n+N_A)}{(N_D-N_A-n)} = \frac{N_C}{2}e^{-E_D/kT}, \tag{13}$$

where k is the Boltzmann constant, T is the temperature, and N_C is the effective density of states in the conduction band of a degenerated semiconductor. Analyses of other samples give similar results.

Thus, besides the line dislocations, donor-type impurities, and point defects can also be considered as a potential source of n-type conductivity. Look *et al.*,[36] by comparing N_D with the concentrations of various donor-type impurities obtained by glow discharge mass spectroscopy analyses, propose hydrogen as a dominant donor in InN epilayers. According to the calculations by Stampfl *et al.*,[72] oxygen acts also as a donor having formation energies significantly lower than a nitrogen vacancy V_N. It has been also calculated that V_N has the lowest energy among native defects in InN, acting as a source of free electrons in as-grown material. However, all these assignment must be considered very tentative. Moreover, impact of impurities and point defects cannot explain observed exponential dependence of the Hall carrier density and the mobility on epilayer thickness. Taking into account all the facts mentioned above, we propose the line dislocation network as a dominant source of electrons and as the main origin of the observed variation of density and mobility of the carriers with the thickness in nominally undoped n-type InN layers ($350 < d < 2200$ nm) grown on AlN(0001) templates.

V. CONCLUSIONS

The microstructure and electron transport properties of heteroepitaxial InN films with varying thickness were analyzed by variable temperature Hall-effect measurements and TEM. The mobility at 300 K was found to be ~1520 cm^2 V^{-1} s^{-1} for the electron concentration of ~9 $\times10^{17}$ cm^{-3}. At 160 K, the mobility reached a maximum of

$\sim$1770 $cm^2\ V^{-1}\ s^{-1}$. It was found that bulk crystal defects (misfit and threading dislocations and DBs) have strong effect on the electron concentration and mobility of the carriers in the InN films. The large lattice mismatch between the epilayer and the substrate results in a high density array of misfit dislocations at the InN/AlN heterointerface and threading dislocations in the bulk of InN epilayers. The threading dislocation density has been found to decay exponentially with epilayer thickness, with the largest proportion being present near the heterointerface causing the observed exponential variations of both the carrier concentration and electron mobility with thickness. The combined analyses of the TEM and Hall data show that the carrier concentration does not have a significant dependence on temperature, regardless of the thickness, presuming a direct dependence between carrier generation and dislocation density in InN films. The variation of mobility with temperature-indicates the dominance of temperature-independent scattering over conventional mechanisms such as ionized impurity and phonon scattering. Among possible origins of the temperature-independent scattering, dislocation strain field scattering has been proposed to be dominant in our 2*H*-InN epilayers. However, neutral and charged impurity scattering also cannot be completely ruled out for thicker epilayers.

More detailed analyses of the electron transport data for the samples prepared at different growth conditions are underway and will help clarify quantitatively the issues related to the origin of a high electron concentration and dominant scattering mechanisms in thicker InN epilayers. The more precise evaluation will require using a variable magnetic field Hall technique.

ACKNOWLEDGMENTS

This work was partly supported by DFG (AM105/1-1, Germany), CICYT (MAT2004-01234, Spain), and EU in the frame of the Sixth Framework Program (NMP4-CT-2003-505641 and NMP4-CT-2004-500101). One of the authors (F.M.M.) would like to thank the Alexander von Humboldt Foundation for the financial support under a Humboldt Research Fellowship SPA/1114640STP.

[1]V. Yu. Davydov *et al.*, Phys. Status Solidi B **229**, R1 (2002).
[2]Z. G. Qian, W. Z. Shen, H. Ogawa, and Q. X. Guo, J. Phys.: Condens. Matter **16**, R381 (2004).
[3]K. S. A. Butcher and T. L. Tansley, Superlattices Microstruct. **38**, 1 (2005).
[4]Q. X. Guo, T. Tanaka, and M. Nishio, Appl. Phys. Lett. **86**, 231913 (2005).
[5]H. L. Xiao, X. L. Wang, J. X. Wang, N. H. Zhang, H. X. Liu, Y. P. Zeng, J. M. Li, and Z. G. Wang, J. Cryst. Growth **276**, 401 (2005).
[6]K. M. Yu *et al.*, Appl. Phys. Lett. **86**, 071910 (2005).
[7]J. Furthmüller, P. H. Hahn, F. Fuchs, and F. Bechstedt, Phys. Rev. B **72**, 205106 (2005).
[8]S. K. O'Leary, B. E. Foutz, M. S. Shur, U. V. Bhapkar, and L. F. Eastman, J. Appl. Phys. **83**, 826 (1998).
[9]B. E. Foutz, S. K. O'Leary, M. S. Shur, and L. F. Eastman, J. Appl. Phys. **85**, 7727 (1999).
[10]I. Vurgaftman and J. R. Meyer, J. Appl. Phys. **94**, 3675 (2003).
[11]S. K. O'Leary, B. E. Foutz, M. S. Shur, and L. F. Eastman, Appl. Phys. Lett. **87**, 222103 (2005).
[12]J. Wu *et al.*, Appl. Phys. Lett. **80**, 3967 (2002).
[13]T. Matsuoka, H. Okamoto, M. Nakao, H. Harima, and E. Kurimoto, Appl. Phys. Lett. **81**, 1246 (2002).
[14]K. Xu and A. Yoshikawa, Appl. Phys. Lett. **83**, 251 (2003).
[15]S. Gwo, C.-L. Wu, C.-H. Shen, W.-H. Chang, T. M. Hsu, J.-S. Wang, and J.-T. Hsu, Appl. Phys. Lett. **84**, 3765 (2004).
[16]A. G. Bhuiyan, A. Hashimoto, and A. Yamamoto, J. Appl. Phys. **94**, 2779 (2003).
[17]B. Monemar, P. P. Paskov, and A. Kasic, Superlattices Microstruct. **38**, 38 (2005).
[18]Y. Saito, N. Teraguchi, A. Suzuki, T. Araki, and Y. Nanishi, Jpn. J. Appl. Phys., Part 2 **40**, L91 (2001).
[19]H. Lu, W. J. Schaff, J. Hwang, H. Wu, G. Koley, and L. F. Eastman, Appl. Phys. Lett. **79**, 1489 (2001).
[20]E. Tiras, D. Zanato, S. Mazzucato, N. Balkan, and W. J. Schaff, Superlattices Microstruct. **36**, 473 (2004).
[21]T. Araki, Y. Saito, T. Yamaguchi, M. Kurouchi, Y. Nanishi, and H. Naoi, J. Vac. Sci. Technol. B **22**, 2139 (2004).
[22]L. F. J. Piper *et al.*, Phys. Rev. B **72**, 245319 (2005).
[23]C.-L. Wu, C.-H. Shen, H.-W. Lin, H.-M. Lee, and S. Gwo, Appl. Phys. Lett. **87**, 241916 (2005).
[24]J. S. Thakur, R. Naik, V. M. Naik, D. Haddad, G. W. Auner, H. Lu, and W. J. Schaff, J. Appl. Phys. **99**, 023504 (2006).
[25]Y. Huang, H. Wang, Q. Sun, J. Chen, D. Y. Li, Y. T. Wang, and H. Yang, J. Cryst. Growth **276**, 13 (2005).
[26]D. A. Neumayer and J. G. Ekerdt, Chem. Mater. **8**, 9 (1996).
[27]A. Yamamoto, M. Tsujino, M. Ohkubo, and A. Hashimoto, J. Cryst. Growth **137**, 415 (1994).
[28]T. Yamaguchi, Y. Saito, C. Morioka, K. Yorozu, T. Araki, A. Suzuki, and Y. Nanishi, Phys. Status Solidi B **240**, 429 (2003).
[29]J. G. Lozano, A. M. Sánchez, R. García, D. González, D. Araújo, S. Ruffenach, and O. Briot, Appl. Phys. Lett. **87**, 263104 (2005).
[30]Y. F. Ng, Y. G. Cao, M. H. Xie, X. L. Xie, X. L. Wang, and S. Y. Tong, Appl. Phys. Lett. **81**, 3960 (2002).
[31]N. Gmeinwieser *et al.*, J. Appl. Phys. **96**, 3666 (2004).
[32]S. F. Chichibu, A. Uedono, T. Onuma, T. Sota, B. A. Haskell, S. P. DenBaars, J. S. Speck, and S. Nakamura, Appl. Phys. Lett. **86**, 021914 (2005).
[33]M. J. Manfra, K. W. Baldwin, A. M. Sergent, K. W. West, R. J. Molnar, and J. Caissie, Appl. Phys. Lett. **85**, 5394 (2004).
[34]Z.-Q. Fang, D. C. Look, D. H. Kim, and I. Adesida, Appl. Phys. Lett. **87**, 182115 (2005).
[35]H. Lu, William J. Schaff, L. S. Eastman, and C. E. Stutz, Appl. Phys. Lett. **82**, 1736 (2003); C. J. Lu, L. A. Bendersky, H. Lu, and William J. Schaff, *ibid.* **83**, 2817 (2003).
[36]D. C. Look, H. Lu, W. J. Schaff, J. Jasinski, and Z. Liliental-Weber, Appl. Phys. Lett. **80**, 258 (2002).
[37]H. Lu, W. J. Schaff, L. F. Eastman, J. Wu, W. Walukiewicz, D. C. Look, and R. J. Molnar, Mater. Res. Soc. Symp. Proc. **743**, L4.10 (2003).
[38]J. Oila *et al.*, Appl. Phys. Lett. **84**, 1486 (2004).
[39]L. H. Dmowski *et al.*, Appl. Phys. Lett. **86**, 262105 (2005).
[40]E. Dimakis, E. Iliopoulos, K. Tsagaraki, Th. Kehagias, Ph. Komninou, and A. Georgakilas, J. Appl. Phys. **97**, 113520 (2005).
[41]V. Gopal, V. Souw, E.-H. Chen, E. P. Kvam, M. McElfresh, and J. M. Woodall, J. Appl. Phys. **87**, 1350 (2000).
[42]V. Lebedev, B. Schröter, G. Kipshidze, and W. Richter, J. Cryst. Growth **207**, 266 (1999).
[43]T. D. Veal, I. Mahboob, L. F. J. Piper, C. F. McConville, H. Lu, and W. J. Schaff, J. Vac. Sci. Technol. B **22**, 2175 (2004).
[44]S. P. Watkins, C. A. Tran, R. Ares, and G. Soerensen, Appl. Phys. Lett. **66**, 882 (1995).
[45]I. Mahboob, T. D. Veal, L. F. J. Piper, C. F. McConville, H. Lu, W. J. Schaff, J. Furthmüller, and F. Bechstedt, Phys. Rev. B **69**, 201307 (2004).
[46]V. Cimalla *et al.*, Phys. Status Solidi A **203**, 59 (2006).
[47]A. F. Wright and U. Grossner, Appl. Phys. Lett. **73**, 2751 (1998).
[48]K. Leung and A. F. Wright, Appl. Phys. Lett. **74**, 2495 (1999).
[49]I. Arslan and N. D. Browning, Phys. Rev. Lett. **91**, 165501 (2003); Phys. Rev. B **65**, 075310 (2002).
[50]D. Cherns and C. G. Jiao, Phys. Rev. Lett. **87**, 205504 (2001).
[51]H. M. Ng, D. Doppalapudi, T. D. Moustakas, N. G. Weimann, and L. F. Eastmann, Appl. Phys. Lett. **73**, 821 (1998).
[52]N. Weimann, L. Eastman, D. Doppalapudi, H. Ng, and T. Moustakas, J. Appl. Phys. **83**, 3656 (1998).
[53]D. C. Look and J. R. Sizelove, Phys. Rev. Lett. **82**, 1237 (1999).
[54]J. W. P. Hsu, M. J. Manfra, S. N. G. Chu, C. H. Chen, L. N. Pfeiffer, and R. J. Molnar, Appl. Phys. Lett. **78**, 3980 (2001).
[55]L. F. J. Piper, T. D. Veal, C. F. McConville, H. Lu, and W. J. Schaff, Appl. Phys. Lett. **88**, 252109 (2006).

[56]C. H. Swartz, R. P. Tompkins, T. H. Myers, H. Lu, and W. J. Schaff, Phys. Status Solidi C **2**, 2250 (2005).
[57]C. H. Swartz, R. P. Tompkins, N. C. Giles, T. H. Myers, H. Lu, W. J. Schaff, and L. F. Eastman, J. Cryst. Growth **269**, 29 (2004).
[58]B. R. Nag, *Electron Transport in Compound Semiconductors* (Springer, New York, 1980), p. 175.
[59]H. Brooks, Adv. Electron. Electron Phys. **7**, 85 (1955).
[60]B. L. Gelmont, M. Shur, and M. Stroscio, J. Appl. Phys. **77**, 657 (1995).
[61]D. C. Look, C. E. Stutz, R. J. Molnar, K. Saarinen, and Z. Liliental-Weber, Solid State Commun. **117**, 571 (2001).
[62]J. E. Dominguez, L. Fu, and X. Q. Pan, Appl. Phys. Lett. **81**, 5168 (2002).
[63]J. M. Ziman, *Electrons and Phonons* (Oxford University Press, London, 1962), p. 428.
[64]L. Solymar and D. Walsh, *Lectures on the Electrical Properties of Materials* (Oxford University Press, London, 1993), p. 163.
[65]S. Kalem, J.-I. Chyi, H. Morkoc, R. Bean, and K. Zanio, Appl. Phys. Lett. **53**, 1647 (1988); S. Kalem, J. Appl. Phys. **66**, 3097 (1988).
[66]Y. Taniyasu, M. Kasu, and T. Makimoto, Appl. Phys. Lett. **85**, 4672 (2004).
[67]V. Gopal, E.-H. Chen, E. P. Kvam, and J. M. Woodall, J. Vac. Sci. Technol. B **17**, 1767 (1999).
[68]H. F. Matare, *Defect Electronic in Semiconductors* (Wiley, New York, 1971), pp. 57–69.
[69]L. L. Kazmerski, W. B. Berry, and C. W. Allen, J. Appl. Phys. **43**, 3515 (1972); **43**, 3521 (1972).
[70]K. Suzuki, M. Ichihara, and S. Takeuchi, Jpn. J. Appl. Phys., Part 1 **33**, 1114 (1994); A. F. Wright, J. Appl. Phys. **82**, 5229 (1997).
[71]M. Fehrer, S. Einfeldt, U. Birkle, T. Gollnik, and D. Hommel, J. Cryst. Growth **189/190**, 763 (1998).
[72]C. Stampfl, C. G. Van de Walle, D. Vogel, P. Krüger, and J. Pollmann, Phys. Rev. B **61**, R7846 (2000).